Electrochemical Oxidation of Diaquaruthenium(II) Complexes of Quaterpyridines and Crystal Structure of $[RuL^1(PPh_3)_2][ClO_4]_2$ (L^1 = 3″,5,5′,5‴-tetramethyl-2,2′:6′,2″:6″,2‴-quaterpyridine)†

Chin-Wing Chan, Ting-Fong Lai and Chi-Ming Che*
Department of Chemistry, The University of Hong Kong, Pokfulam Road, Hong Kong

The perchlorate salts of $[RuL^2(OH_2)_2]^{2+}$ **1** and $[RuL^1(OH_2)_2]^{2+}$ **2** (L^2 = 2,2′:6′,2″:6″,2‴-quaterpyridine, L^1 = 3″,5,5′,5‴-tetramethyl-2,2′:6′,2″:6″,2‴-quaterpyridine) have been isolated. In acidic solutions both **1** and **2** exhibit reversible Ru^{VI}–Ru^{IV} and Ru^{III}–Ru^{II} couples, though the Ru^{IV}–Ru^{III} couples are only quasireversible. The effect of pH on the $E_{\frac{1}{2}}$ of these couples has been investigated. At pH 1, the $E°$ values of the $[RuL^2O_2]^{2+}$–$[RuL^2(O)(OH_2)]^{2+}$ and $[RuL^1O_2]^{2+}$–$[RuL^1(O)(OH_2)]^{2+}$ couples are 1.12 and 1.05 V *vs.* saturated calomel electrode respectively. The crystal structure of $[RuL^1(PPh_3)_2][ClO_4]_2 \cdot MeCN \cdot H_2O$ has been determined: monoclinic space group $P2_1/n$, a = 13.210(4), b = 29.711(7), c = 14.878(3) Å, β = 98.89(2)°, Z = 4. In this complex the quaterpyridine ligand adopts a non-planar conformation with a dihedral angle of 28.3° between the two central pyridyl rings. The two triphenylphosphine ligands are in a *trans* configuration [P(1)–Ru–P(2) 177.6°]. The complex $[RuL^2(OH_2)_2]^{2+}$ is an active catalyst for the electrochemical oxidation of propan-2-ol.

Ruthenium occupies its special niche in redox chemistry because a repertoire of oxidation states are accessible within a narrow potential range from diaquaruthenium(II). The complex *trans*-$[Ru(tmc)O_2]^{2+}$ (tmc = 1,4,8,11-tetramethyl-1,4,8,11-tetraazacyclotetradecane)[1] could be generated at 0.66 V (*vs.* saturated calomel electrode, SCE) in pH 1 aqueous solution. Under the same conditions, incorporation of chelating pyridyl groups into the co-ordination sphere of ruthenium would increase the $E°$ of *trans*-dioxoruthenium(VI) to 0.89 V (*vs.* SCE) in $[RuLO_2]^{2+}$ [L = *N,N′*-dimethyl-*N,N′*-bis(2-pyridylmethyl)propylenediamine][2] and even 1.01 V in $[Ru(bipy)_2O_2]^{2+}$ (bipy = 2,2′-bipyridine).[3] These high-valent oxo-ruthenium species have been shown to be competent oxidants for organic oxidation.[4,5]

We have been interested in investigating the photophysical and electrochemical properties of transition-metal complexes containing polypyridine ligands. In this context, the two tetradentate chelating ligands 3″,5,5′,5‴-tetramethyl-2,2′:6′,2″:6″,2‴-quaterpyridine (L^1)[6] and 2,2′:6′,2″:6″,2‴-quaterpyridine (L^2)[7] are of interest to us. Previous studies by Lehn,[6] Constable,[7] and Che[8] and their co-workers have demonstrated the versatile co-ordination chemistry of L^1 and L^2. We expect that dioxoruthenium(VI) complexes of these ligands, if generated, are strongly oxidizing and may be stable with regard to ligand dissociation. Herein is described the synthesis and electrochemistry of *trans*-$[Ru^{II}L^2(OH_2)_2]^{2+}$ and *trans*-$[Ru^{II}L^1(OH_2)_2]^{2+}$ and the X-ray crystal analysis of *trans*-$[Ru^{II}L^1(PPh_3)_2][ClO_4]_2$.

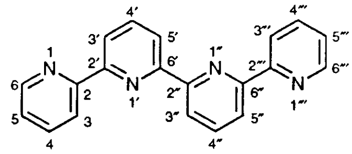

2, 2′:6′, 2″:6″, 2‴-quaterpyridine

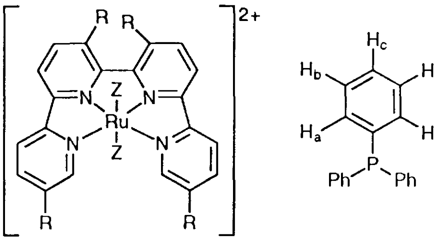

R = H or Me
Z = MeCN, H_2O, or PPh_3

Experimental

Materials.—The quaterpyridines L^1 (ref. 6) and L^2 [ref. 7(*a*)] were prepared as described, as were $[Ru(OH_2)_6][p\text{-}MeC_6H_4SO_3]_2$[9] and $[Ru(PPh_3)_2(MeCO_2)_2]$.[10] All chemicals were of analytical grade and used as received. Water for electrochemical studies was distilled twice from $KMnO_4$, and acetonitrile successively from $KMnO_4$ and CaH_2.

Physical Measurements and Instrumentation.—Infrared spectra were measured on a Nicolet 20 SXC FT-IR spectrometer, UV/VIS spectra on a Milton Roy Spectronic 3000 spectrophotometer and ^1H NMR spectra on a JEOL GSX 270 FT-NMR spectrometer with $SiMe_4$ as internal standard. Elemental analyses were performed by the Shanghai Institute of Organic Chemistry, Chinese Academy of Science and the Department of Chemistry at National Taiwan University.

Cyclic voltammograms were measured using a Princeton Applied Research (PAR) model 273 potentiostat and recorded on a Kipp & Zonen X-Y recorder. A conventional two-compartment cell was used in all measurements. The working edge-plane pyrolytic graphite and auxiliary platinum electrodes were separated from the saturated calomel electrode by a

---

† *Supplementary data available:* see Instructions for Authors, *J. Chem. Soc., Dalton Trans.*, 1994, Issue 1, pp. xxiii–xxviii.

sintered-glass disc. The surface of the graphite electrode was treated as described before.[11] The potentials ($E°$) of all reversible couples were reported as estimates of $(E_{pa} + E_{pc})/2$, and the E_{pa} values were recorded for irreversible electrode processes.

Crystal Structure Determination.—Crystal data. $C_{60}H_{52}Cl_2N_4O_8P_2Ru{\cdot}MeCN{\cdot}H_2O$, $M = 1250.09$, monoclinic, space group $P2_1/n$, $a = 13.210(4)$, $b = 29.711(7)$, $c = 14.878(3)$ Å, $\beta = 98.89(2)°$, $U = 5769(4)$ Å^3, $T = 296$ K, $D_m = 1.45$ g cm^{-3}, $Z = 4$, $D_c = 1.44$ g cm^{-3}, $F(000) = 2576$, μ(Mo-Kα) = 4.73 cm^{-1}. Crystal dimensions 0.07 × 0.21 × 0.35 mm.

Data collection and processing. A dark red prism of $[RuL^1(PPh_3)_2][ClO_4]_2$ was obtained by slow evaporation of an acetonitrile solution of the complex at room temperature. Diffraction data were collected on an Enraf-Nonius CAD4 diffractometer (graphite-monochromated Mo-Kα radiation, $\lambda = 0.71073$ Å) in ω–2θ mode. The unit-cell dimensions were obtained from a least-squares fit of 25 reflections in the range $20 < 2\theta < 30°$. Of 11801 data collected (at $2\theta_{max} = 52°$ and range $hk \pm l$), 11288 were considered unique. The data were corrected for Lorentz and polarization effects, but not for absorption. Three reflections were monitored every 2 h, but showed no significant variation in intensity. Calculations were carried out on 7627 reflections $[m, F_o > 3\sigma(F_o)]$ and 698 parameters (p) with a Micro Vax II computer using the Enraf-Nonius SDP programs.[12] The position of the ruthenium atom was obtained from a Patterson synthesis, and the rest of the non-hydrogen atoms were located from subsequent Fourier maps. Refinement was by full-matrix least squares with a weighting scheme $w = 4F_o^2/[\sigma^2(F_o^2) + (0.055F_o^2)^2]$. One of the perchlorate groups was disordered and appeared to rotate about one of its Cl–O bonds. The three disordered oxygen atoms were located at six idealized sites from a Fourier difference map, each with an occupancy factor of 0.5, and their parameters were not adjusted in subsequent refinement. During the final least-squares cycles all non-hydrogen atoms except the oxygen atom in the water molecule were refined anisotropically. The final agreement factors $R(F_o) = \Sigma||F_o| - |F_c||/\Sigma|F_o|$, $R' = [\Sigma w(|F_o| - |F_c|)^2/\Sigma w|F_o|^2]^{\frac{1}{2}}$ and $S = [\Sigma w(|F_o| - |F_c|)^2/(m - p)]^{\frac{1}{2}}$ were 0.058, 0.080, and 1.96, respectively. The hydrogen atoms in the methyl groups and water molecule were omitted while all other hydrogen atoms at calculated positions were included in the structure-factor calculation. The final Fourier difference map contained extrema at 1.89 and −1.00 e Å^{-3}. Table 1 lists the atomic coordinates for the non-hydrogen atoms, Table 2 selected bond distances and angles.

Additional material available from the Cambridge Crystallographic Data Centre comprises H-atom coordinates, thermal parameters and remaining bond lengths and angles.

Synthesis.—$[RuL^2(OH_2)_2][ClO_4]_2$ **1**. A solution of $[Ru(OH_2)_6][p\text{-}MeC_6H_4SO_3]_2$ (50 mg, 9.1×10^{-5} mol) and L^2 (40.4 mg, 1.4 equivalents) in degassed 95% ethanol (100 cm^3) was refluxed under a nitrogen atmosphere for 3 h. The bluish purple solution was filtered while warm, treated with an excess of sodium perchlorate, concentrated to about 10 cm^3 under reduced pressure, and kept at 4 °C for 2 h. A purple solid (23 mg) was isolated in 27% yield (Found: C, 37.4; H, 3.1; N, 8.3. Calc. for $C_{20}H_{18}Cl_2N_4O_{10}Ru$: C, 37.15; H, 2.80; N, 8.65%). IR (cm^{-1}): 3439s, 1143s, 1120s, 1088s, 769s, 639m and 627m. UV/VIS in 0.1 mol dm^{-3} CF_3CO_2H (λ_{max}/nm, $10^{-3}\varepsilon$/dm^3 mol^{-1} cm^{-1}): 281 (24.3), 291 (26.6), 320 (23.7), 348 (8.4), 480 (2.8) and 552 (2.8).

$[RuL^1(OH_2)_2][ClO_4]_2$ **2**. The above procedure was adopted except that L^1 was used. Yield 22%. IR (cm^{-1}): 3439s, 2980w, 1143s, 1120s, 1088s, 769s, 639m and 627m. UV/VIS in 0.1 mol dm^{-3} CF_3CO_2H (λ_{max}/nm, $10^{-3}\varepsilon$/dm^3 mol^{-1} cm^{-1}): 300 (20), 330 (20), 355 (8), 460 (3) and 550 (3).

$[RuL^1(PPh_3)_2][ClO_4]_2$ **3**. A mixture of diacetatobis(triphenylphosphine)ruthenium(II) (222 mg, 3×10^{-4} mol) and L^1 (100 mg, 2.73×10^{-4} mol) in degassed methanol (120 cm^3) was stirred under a nitrogen atmosphere at room temperature for 45 h. The reddish solution was filtered promptly, treated with an excess of lithium perchlorate, and concentrated to about 50 cm^3 under reduced pressure. The microcrystals formed were filtered off, washed with a few cm^3 of cold methanol and dried under reduced pressure. Yield 72% (Found: C, 60.3; H, 4.05; N, 4.60. Calc. for $C_{60}H_{52}Cl_2N_4O_8P_2Ru$: C, 60.50; H, 4.40; N, 4.70%). ^{1}H NMR (CD_3CN): δ 9.74 (s, $H^{6,6'''}$), 7.60–7.31 (m, $H^{3,4,3',4',4'',5'',3''',4'''}$), 7.43–7.35 (m, H_c), 7.15–7.09 (t, H_b), 6.67–6.60 (m, H_a), 2.49 (s, 5′- and 3″-CH_3), and 2.40 (s, 5- and 5‴-CH_3). IR (cm^{-1}): 1483w, 1120m, 1089s, 700m, 624m and 517m. UV/VIS in MeCN (λ_{max}/nm, $10^{-3}\varepsilon$/dm^3 mol^{-1} cm^{-1}): 267 (76), 297 (35), 312 (35), 344 (18), 358 (24), 415 (4.1) and 450 (4).

$[RuL^2(PPh_3)_2][ClO_4]_2$ **4**. The above procedure for preparation of complex **3** was adopted except that L^2 was used. Yield was 33%. ^{1}H NMR (CD_3CN): δ 9.93–9.53 (m, $H^{6,6'''}$) and 8.17–6.55 (m, C_6H_5 and $H^{3-5,3'-5',3''-5'',3'''-5'''}$) (Found: C, 58.9; H, 4.1; N, 4.8. Calc. for $C_{56}H_{44}Cl_2N_4O_8P_2Ru$: C, 59.25; H,3.90; N, 4.95%). IR (cm^{-1}): 1476m, 1144s, 1120s, 1108s, 775m, 749m, 699m, 624m and 518m. UV/VIS in MeCN (λ_{max}/nm, $10^{-3}\varepsilon$/dm^{-3} mol^{-1} cm^{-1}): 268 (33), 288 (26), 333 (12), 348 (14), 416 (2.8), 463 (3.4) and 523 (2.0).

$[RuL^2(MeCN)_2][ClO_4]_2$ **5**. The compound L^2 (52 mg, 1.7×10^{-4} mol) and $[Ru(OH_2)_6][p\text{-}MeC_6H_4SO_3]_2$ (88 mg, 1.0×10^{-4} mol) were refluxed in degassed acetone–methanol (1 : 1 v/v, 50 cm^3) for 48 h. The solution was reduced to half its original volume under reduced pressure. A black solid was filtered off, redissolved in acetonitrile and treated with an excess of lithium perchlorate. Recrystallization by ether diffusion afforded dark red needles (23 mg) in 20% yield (Found: C, 41.55; H, 2.90; N, 12.00. Calc. for $C_{24}H_{20}Cl_2N_6O_8Ru$: C, 41.60; H, 2.90; N, 12.15%). ^{1}H NMR (CD_3CN): δ 9.40 (ddd, $H^{6,6'''}$), 8.42 (dd, $H^{3',5',3'',5''}$), 8.35–8.32 (dd, $H^{3,3'''}$), 8.27 (td, $H^{4,4'''}$), 8.15 (t, $H^{4',4''}$), 7.87 (ddd, $H^{5,5'''}$) and 1.79 (s, CH_3CN). IR (cm^{-1}): 1105s, 1089s, 768s and 623s. UV/VIS in MeCN (λ_{max}/nm, $10^{-3}\varepsilon$/dm^3 mol^{-1} cm^{-1}): 283 (42.1), 327 (15.1), 342 (20.0), 376 (1.8), 420 (3.2), 476 (5.0) and 501 (4.3).

Results and Discussion

Properties, Crystal and Molecular Structure.—There have been a number of studies on 2,2′:6′,2″:6″,2‴-quaterpyridine complexes.[7,8] Although considerable strain in the planar tetradentate co-ordination mode has been noted in transition-metal complexes,[7,8] isolation of ruthenium(II) quaterpyridine complexes is possible with $[Ru(OH_2)_6]^{2+}$ and $[Ru(MeCO_2)_2(PPh_3)_2]$ as starting materials.

Both $[RuL^1(OH_2)_2][ClO_4]_2$ and $[RuL^2(OH_2)_2][ClO_4]_2$ are less stable than expected. Attempts to grow suitable crystals of *trans*-$[RuL^2(OH_2)_2][ClO_4]_2$ for X-ray crystal analysis were unsuccessful. Solid samples of the diaqua complexes are susceptible to air oxidation especially in the presence of moisture. Purple solutions of these complexes turn brownish green when exposed to air within a few hours. This is not unexpected since the related *trans*-$[Ru(bipy)_2(OH_2)_2]^{2+}$ complex is unstable upon prolonged storage.[13]

The first unequivocal evidence for the tetradentate co-ordination mode of L^2 came from the crystal analysis of $[CoL^2(OH_2)(SO_3)]NO_3{\cdot}H_2O$.[14] In contrast, the methyl groups in L^1 should prevent it from acting as a planar tetradentate ligand as in the case of $[Cu_2L^1][ClO_4]_2{\cdot}H_2O$.[6] Tetradentate co-ordination of L^1 is possible when there are strong metal–ligand interactions as in the case of $[PtL^1]^{2+}$.[8a] To our knowledge, no crystal structure has been reported on mononuclear ruthenium(II) complexes of L^1 or L^2. That described here consists of, in addition to quaterpyridine, two bulky triphenylphosphine ligands in a *trans* configuration. A perspective view of the complex cation $[RuL^1(PPh_3)_2]^{2+}$ is shown in Fig. 1. The two bipyridyl units are twisted with a

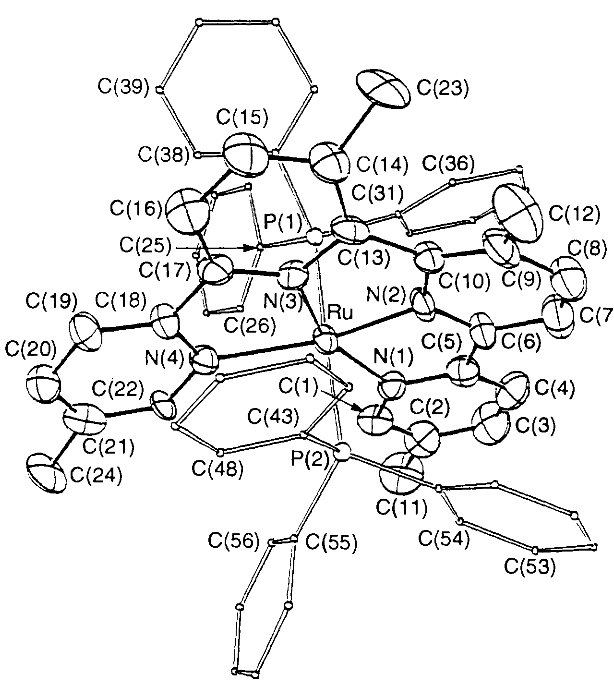

Fig. 1 Perspective view of $[RuL^1(PPh_3)_2][ClO_4]_2$

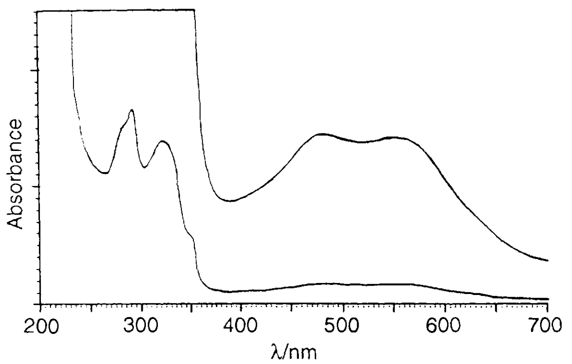

Fig. 2 The UV/VIS spectrum of $[RuL^2(OH_2)_2]^{2+}$ in 0.1 mol dm^{-3} CF_3CO_2H aqueous solution

dihedral angle of ≈28°, indicating the inherent instability of L^1 in the tetradentate co-ordination mode. On the other hand, the two bulky phosphine ligands only slightly deviate from a *trans* configuration [P(1)–Ru–P(2) 177.6°].

The UV/VIS absorption spectra of all ruthenium(II) quaterpyridine complexes are similar. Basically, there are intense intraligand transitions around 300 nm ($\varepsilon > 10^4$ dm^3 mol^{-1} cm^{-1}) and metal-to-ligand charge transfer (m.l.c.t.) transitions from 400 to 500 nm ($\varepsilon > 10^3$ dm^3 mol^{-1} cm^{-1}) (Fig. 2). The positions of the absorption bands for complexes **1** and **2** are similar to those of *trans*-$[Ru(bipy)_2(OH_2)_2]^{2+}$.[13]

Electrochemical Studies.—Electrooxidation of *trans*-diaquaruthenium(II) complexes in aqueous media have been well documented.[2,3] In aqueous media both $[RuL^2(OH_2)_2]^{2+}$ and $[RuL^1(OH_2)_2]^{2+}$ display very similar cyclic voltammograms to those of *trans*-$[Ru(tmc)O_2]^{2+}$ and *trans*-$[Ru(bipy)_2(OH_2)]^{2+}$ except with a shift in $E_{\frac{1}{2}}$ values. Fig. 3 shows the cyclic voltammogram of complex **1** in pH 1 solution. As for the oxidation of *trans*-diaquaruthenium(II) to *trans*-dioxoruthenium(VI), there are three reversible couples: I, at 0.58 V with a peak-to-peak separation (ΔE_p) ≈50 mV, II at 0.91 V with ΔE_p > 100 mV, and III at 1.12 V with ΔE_p 30–40 mV. For complex **2** in pH 1 solution, the corresponding three redox couples are at 0.46, 0.90 and 1.05 V.

Studies on the effect of pH on $E_{\frac{1}{2}}$ values revealed that these are all proton-coupled electron-transfer processes. The Pourbaix diagrams shown in Fig. 4(*a*) and 4(*b*) cover the pH range from 1 to 9 for complex **1** and from 1 to 10 for **2**. Since both **1** and **2** are unstable in aqueous solution upon prolonged standing, we found it very difficult to determine the *n* values of the redox couples I–III by coulometric experiments. However, with reference to previous studies on the well established *trans*-dioxoruthenium(VI) systems, these couples can be assigned as in equations (1)–(5). As expected the $E°$ values are almost constant from pH 1 to 1.4 for **1** and **2**. At pH 1.4–6.0, the best straight lines for $E°$ values have slopes of −56 and −60 mV per pH unit for **1** and **2**, respectively. This accounts for a one proton–one electron couple. At pH ≥6, the slopes change to −118 mV per pH unit for **1** and **2**, suggesting a two proton–one electron couple [equation (3)]. Couple II is assigned to the one proton–one electron oxidation of Ru^{III} to Ru^{IV} where the best straight lines in the Pourbaix diagram from pH 1 to 6 have slopes of −59 and −66 mV per pH unit for **1** and **2**, respectively. Couple III is assigned to a two proton–two electron oxidation of Ru^{IV} to Ru^{VI} based on the smaller value of ΔE_p (≈30–40 mV) and previous studies on related systems such as *trans*-$[Ru(bipy)_2(OH_2)_2]^{2+}$. Furthermore, the peak height for couple III is much larger than those of I or II. In the Pourbaix

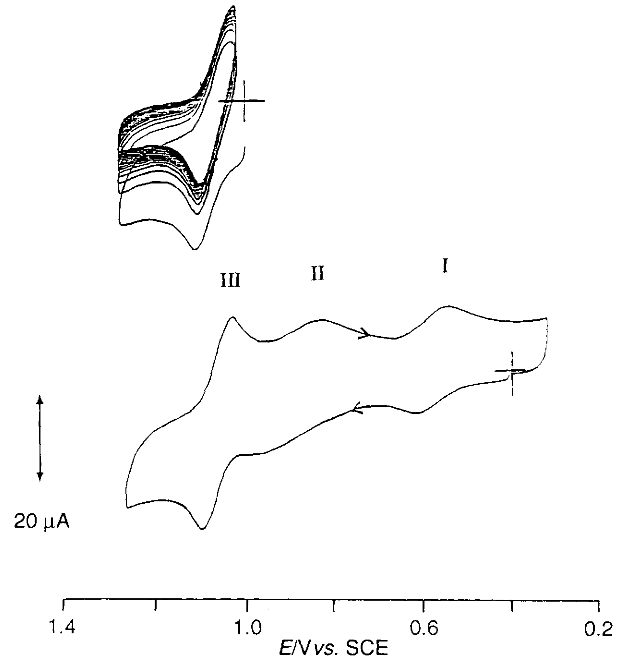

Fig. 3 Cyclic voltammogram of $[RuL^2(OH_2)_2]^{2+}$ in 0.1 mol dm^{-3} CF_3CO_2H aqueous solution. Insert: repeat cycling between 1.0 and 1.3 V; scan rate 50 mV s^{-1}

Couple Ia (pH ≈1):

$$[Ru^{III}L(OH_2)_2]^{3+} + e \longrightarrow [Ru^{II}L(OH_2)_2]^{2+} \quad (1)$$

Couple Ib (pH 1.4–6.0):

$$[Ru^{III}L(OH)(OH_2)]^{2+} + e + H^+ \longrightarrow [Ru^{II}L(OH_2)_2]^{2+} \quad (2)$$

Couple Ic (pH ≥6):

$$[Ru^{III}L(OH)_2]^{+} + e + 2H^+ \longrightarrow [Ru^{II}L(OH_2)_2]^{2+} \quad (3)$$

Couple II (pH 1–6):

$$[Ru^{IV}L(O)(OH_2)]^{2+} + e + H^+ \longrightarrow [Ru^{III}L(OH)(OH_2)]^{2+} \quad (4)$$

Couple III (pH 1–6):

$$[Ru^{VI}LO_2]^{2+} + 2e + 2H^+ \longrightarrow [Ru^{IV}L(O)(OH_2)]^{2+} \quad (5)$$

Table 1 Fractional atomic coordinates of non-hydrogen atoms with their estimated standard deviations in parentheses for $[RuL^1(PPh_3)_2][ClO_4]_2$

Atom	*x*	*y*	*z*	Atom	*x*	*y*	*z*
Ru	0.161 10(3)	0.133 33(1)	0.294 60(3)	C(36)	0.339 5(5)	0.070 7(2)	0.133 7(4)
P(1)	0.173 0(1)	0.130 28(5)	0.134 88(9)	C(37)	0.241 3(5)	0.177 1(2)	0.090 9(4)
P(2)	0.151 5(1)	0.133 13(5)	0.455 42(9)	C(38)	0.193 5(5)	0.218 7(2)	0.088 0(4)
N(1)	0.114 3(3)	0.063 8(1)	0.283 3(3)	C(39)	0.238 8(7)	0.256 5(2)	0.055 1(5)
N(2)	0.294 3(3)	0.102 2(1)	0.321 9(3)	C(40)	0.332 3(6)	0.252 7(3)	0.025 3(5)
N(3)	0.252 8(3)	0.186 4(1)	0.309 3(3)	C(41)	0.378 5(6)	0.211 5(3)	0.027 6(5)
N(4)	0.052 7(3)	0.189 0(1)	0.280 1(3)	C(42)	0.335 0(5)	0.173 6(2)	0.060 0(5)
C(1)	0.022 8(4)	0.044 4(2)	0.257 8(4)	C(43)	0.212 0(4)	0.184 1(2)	0.506 0(4)
C(2)	0.007 3(5)	−0.001 8(2)	0.248 9(4)	C(44)	0.318 8(5)	0.188 5(2)	0.524 1(4)
C(3)	0.093 9(5)	−0.029 2(2)	0.268 6(5)	C(45)	0.363 4(6)	0.230 1(3)	0.547 1(5)
C(4)	0.187 0(5)	−0.011 0(2)	0.295 9(4)	C(46)	0.300 8(7)	0.267 2(2)	0.549 9(5)
C(5)	0.198 3(4)	0.035 7(2)	0.303 5(4)	C(47)	0.195 6(7)	0.263 5(2)	0.534 1(5)
C(6)	0.297 7(4)	0.057 3(2)	0.331 9(4)	C(48)	0.151 7(5)	0.222 3(2)	0.511 6(4)
C(7)	0.390 4(5)	0.036 9(2)	0.368 1(4)	C(49)	0.205 6(4)	0.083 6(2)	0.517 9(4)
C(8)	0.471 0(5)	0.063 9(2)	0.397 6(5)	C(50)	0.299 9(5)	0.081 1(2)	0.576 7(5)
C(9)	0.469 0(4)	0.110 5(2)	0.387 6(4)	C(51)	0.332 2(5)	0.041 1(3)	0.617 0(5)
C(10)	0.379 1(4)	0.129 7(2)	0.342 1(4)	C(52)	0.274 9(6)	0.002 7(2)	0.602 1(5)
C(11)	−0.099 6(5)	−0.021 0(2)	0.218 3(6)	C(53)	0.180 4(6)	0.004 1(2)	0.545 0(5)
C(12)	0.560 7(5)	0.139 1(3)	0.434 9(6)	C(54)	0.148 7(5)	0.044 4(2)	0.502 9(4)
C(13)	0.355 7(4)	0.177 2(2)	0.317 8(4)	C(55)	0.025 7(4)	0.133 1(2)	0.492 1(4)
C(14)	0.421 8(4)	0.211 9(2)	0.300 0(4)	C(56)	−0.060 4(4)	0.119 4(2)	0.433 0(4)
C(15)	0.380 5(5)	0.255 3(2)	0.293 5(5)	C(57)	−0.155 0(4)	0.115 9(2)	0.462 1(4)
C(16)	0.280 3(4)	0.264 1(2)	0.297 5(5)	C(58)	−0.163 5(5)	0.125 4(2)	0.550 7(4)
C(17)	0.214 5(4)	0.227 8(2)	0.300 6(4)	C(59)	−0.079 4(5)	0.138 5(2)	0.610 9(4)
C(18)	0.102 1(4)	0.229 7(2)	0.291 4(3)	C(60)	0.016 6(5)	0.142 7(2)	0.582 7(4)
C(19)	0.050 6(4)	0.269 4(2)	0.294 9(4)	Cl(1)	0.685 0(1)	0.091 91(6)	0.186 4(1)
C(20)	−0.056 0(5)	0.268 8(2)	0.290 2(4)	Cl(2)	0.599 5(1)	0.112 61(6)	0.703 5(1)
C(21)	−0.106 9(4)	0.228 9(2)	0.280 1(4)	O(11)	0.681 2(7)	0.054 4(3)	0.134 1(5)
C(22)	−0.049 7(4)	0.189 6(2)	0.273 5(4)	O(12)	0.787 0(5)	0.097 6(3)	0.231 0(6)
C(23)	0.528 5(5)	0.204 9(3)	0.277 9(5)	O(13)	0.622 0(5)	0.088 6(3)	0.252 0(5)
C(24)	−0.223 1(4)	0.224 9(3)	0.276 5(5)	O(14)	0.655 4(8)	0.128 7(3)	0.132 2(5)
C(25)	0.056 0(4)	0.129 9(2)	0.051 2(4)	O(21)	0.600 6(5)	0.078 2(2)	0.638 3(5)
C(26)	−0.038 0(5)	0.121 3(2)	0.075 2(4)	O(22)*	0.659 6	0.101 6	0.784 3
C(27)	−0.125 1(5)	0.117 5(2)	0.009 3(5)	O(23)*	0.636 5	0.151 6	0.672 5
C(28)	−0.115 2(6)	0.122 4(2)	−0.081 0(5)	O(24)*	0.493 2	0.120 1	0.718 6
C(29)	−0.021 3(7)	0.132 2(3)	−0.104 6(5)	O(22′)*	0.529 9	0.148 3	0.663 2
C(30)	0.065 2(6)	0.136 0(2)	−0.040 2(4)	O(23′)*	0.559 6	0.095 5	0.782 1
C(31)	0.235 6(4)	0.078 6(2)	0.105 8(4)	O(24′)*	0.694 8	0.127 9	0.732 9
C(32)	0.177 0(6)	0.044 0(2)	0.060 8(4)	N(5)	0.232 4(8)	0.139 0(4)	0.790 3(7)
C(33)	0.224 0(7)	0.003 5(2)	0.044 1(5)	C(61)	0.353(1)	0.077 3(6)	0.866 3(9)
C(34)	0.326 3(8)	−0.003 0(3)	0.070 9(6)	C(62)	0.293 0(9)	0.109 9(5)	0.827 9(7)
C(35)	0.384 8(6)	0.030 4(3)	0.115 8(5)	O	0.056(1)	0.362 5(6)	0.449(1)

* Occupancy factor = 0.5.

Table 2 Selected bond lengths (Å) and angles (°) for $[RuL^1(PPh_3)_2][ClO_4]_2$

Ru-P(1)	2.407(1)	P(1)-Ru-P(2)	177.60(5)
Ru-P(2)	2.416(1)	N(1)-Ru-N(3)	159.2(2)
Ru-N(1)	2.155(5)	N(1)-Ru-N(4)	123.0(2)
Ru-N(2)	1.973(4)	N(2)-Ru-N(3)	80.7(2)
Ru-N(3)	1.979(4)	N(2)-Ru-N(4)	158.2(2)
Ru-N(4)	2.176(4)	N(3)-Ru-N(4)	77.8(2)

diagram, the best straight lines from pH 1 to 6 have slopes of −58 and −55 mV per pH unit for **1** and **2**, respectively. The observed $E_{\frac{1}{2}}(Ru^{VI}-Ru^{IV})$ of $[RuL^2O_2]^{2+}$ at 1.12 V (in pH 1 solution) is the highest ever reported for *trans*-dioxoruthenium(VI).[2,3] For complex **2** $E_{\frac{1}{2}}(Ru^{VI}-Ru^{IV})$ is observed at 1.05 V (in pH 1 solution).

It is interesting that the high-valent oxoruthenium species generated by electrochemical oxidation of complex **1** in acidic media are considerably more stable than that of **2**. Repeated cycling of the former between 1.0 and 1.3 V shows no significant deterioration of couple III (insert of Fig. 3). However, repetitive cyclic voltammetric scans of **2** in aqueous solutions revealed a faster rate of decomposition of $[RuL^1O_2]^{2+}$. This suggests that the twisted conformation of L^1 is also unfavourable for *trans*-dioxoruthenium(VI).

In basic solutions, cyclic voltammetric studies of complexes **1** and **2** are complicated. Couples II and III become ill defined and the complexes were found to degrade fairly rapidly. Nevertheless, the $Ru^{III}-Ru^{II}$ couple is still reversible and its $E_{\frac{1}{2}}$ can be measured.

The planar aromaticity of co-ordinated quaterpyridine, as revealed by crystal analysis, is an important property for fabrication of chemically modified electrodes. Complex **1** was found to adsorb on edge-plane pyrolytic graphite.[15] Fig. 5 shows the cyclic voltammogram of such an electrode in pH 1.4 $Na(O_2CCF_3)-CF_3CO_2H$ buffer after it had been cycled in $\approx 10^{-5}$ mol dm^{-3} **1** and washed subsequently with a stream of distilled water. The redox couples are due to complex **1** adsorbed on the surface of the electrode. With the addition of $\approx 10^{-4}$ mol dm^{-3} propan-2-ol a large catalytic current is generated at about 1 V where a very small current was observed in the absence of the adsorbed ruthenium complex under similar conditions.

In the presence of four methyl groups in the 3″,5,5′,5‴ positions no surface adsorption of complex **2** is observed. Although structural data for **2** are not available, it can be inferred that the co-ordinated ligand L^1 probably has a non-planar conformation similar to that in **3**. Such a conformation is expected not to favour adsorption of the ruthenium complex on the electrode surface.

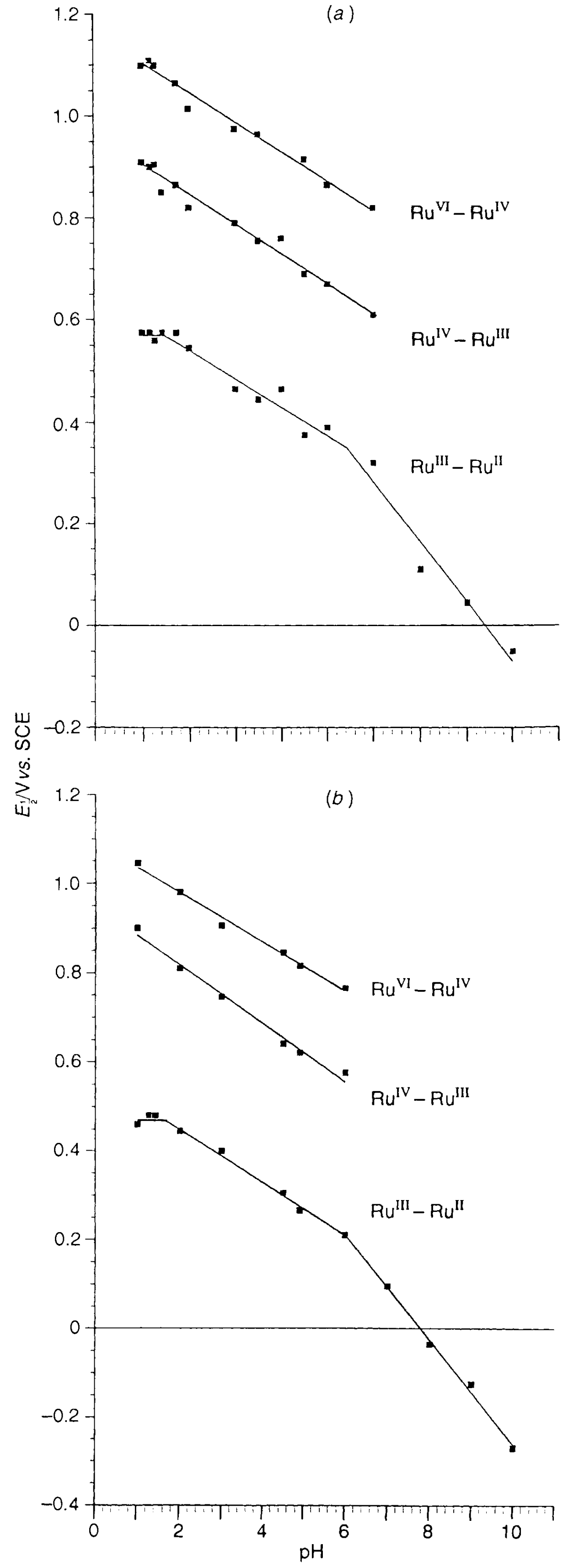

Fig. 4 Pourbaix diagrams for (*a*) $[RuL^2(OH_2)_2]^{2+}$ and (*b*) $[RuL^1(OH_2)_2]^{2+}$

Acknowledgements

We acknowledge support from The Hong Kong Research Grants Council and The University of Hong Kong. C.-W. C. is grateful for the award of a Hung Hing-Ying Scholarship (1992–1993) administered by The University of Hong Kong.

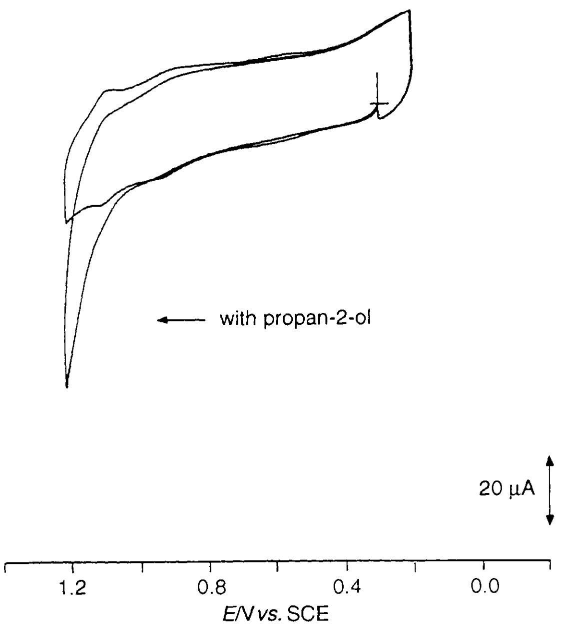

Fig. 5 Residual current from surface-adsorbed $[RuL^2(OH_2)_2]^{2+}$ on edge-plane pyrolytic graphite and catalytic current resulting from oxidation of propan-2-ol ($\approx 10^{-4}$ mol dm^{-3}). Measurements were taken in a mixture of 0.04 mol dm^{-3} CF_3CO_2H and 0.06 mol dm^{-3} $Na(O_2CCF_3)$ aqueous solution with scan rate of 50 mV s^{-1}

References

1 C. M. Che, K. Y. Wong and C. K. Poon, *Inorg. Chem.*, 1985, **24**, 1797.
2 C. M. Che, W. T. Tang and C. K. Li, *J. Chem. Soc., Dalton Trans.*, 1990, 3735.
3 C. M. Che, K. Y. Wong, W. H. Leung and C. K. Poon, *Inorg. Chem.*, 1986, **25**, 345; J. C. Dobson and T. J. Meyer, *Inorg. Chem.*, 1988, **27**, 3283.
4 C. M. Che, W. H. Leung, C. K. Li and C. K. Poon, *J. Chem. Soc., Dalton Trans.*, 1991, 379; C. M. Che, C. Ho and T. C. Lau, *J. Chem. Soc., Dalton Trans.*, 1991, 1259.
5 W. P. Griffith, *Chem. Soc. Rev.*, 1992, **21**, 179.
6 J. M. Lehn, J. P. Sauvage, J. Simon, R. Ziessel, C. Piccini Leopardi, G. Germain, J.-P. Declercq and M. Van Meersche, *Nouv. J. Chim.*, 1983, **7**, 413.
7 (*a*) E. C. Constable, S. M. Elder, J. Healy and D. A. Tocher, *J. Chem. Soc. Dalton Trans.*, 1990, 1669; (*b*) E. C. Constable, S. M. Elder and D. A. Tocher, *Polyhedron*, 1992, **11**, 1337; (*c*) E. C. Constable, S. M. Elder, J. Healy and M. D. Ward, *J. Am. Chem. Soc.*, 1990, **112**, 4590.
8 (*a*) C. W. Chan, C. M. Che, M. C. Cheng and Y. Wang, *Inorg. Chem.*, 1992, **31**, 4874; (*b*) C. M. Che, Y. P. Wang, K. S. Yeung, K. Y. Wong and S. M. Peng, *J. Chem. Soc., Dalton Trans.*, 1992, 2675; (*c*) S. M. Yang, K. K. Cheung and C. M. Che, *J. Chem. Soc., Dalton Trans.*, 1993, 3515.
9 P. Bernhard, H.-B. Bürgi, J. Hauser, H. Lehmann and A. Ludi, *Inorg. Chem.*, 1982, **21**, 3936.
10 R. W. Mitchell, A. Spencer and G. Wilkinson, *J. Chem. Soc., Dalton Trans.*, 1973, 846.
11 C. M. Che, K. Y. Wong and F. C. Anson, *J. Electroanal. Chem. Interfacial Electrochem.*, 1987, **226**, 211.
12 Enraf-Nonius Structure Determination Package, Enraf-Nonius, Delft, 1985.
13 B. Durham, S. R. Wilson, D. J. Hodgson and T. J. Meyer, *J. Am. Chem. Soc.*, 1980, **102**, 600.
14 E. N. Maslen, C. L. Raston and A. H. White, *J. Chem. Soc., Dalton Trans.*, 1975, 323.
15 K. Y. Wong, W. O. Lee, C. M. Che and F. C. Anson, *J. Electroanal. Chem. Interfacial Electrochem.*, 1991, **319**, 207 and refs. therein.

Received 29*th October* 1993; *Paper* 3/06481F